Azimuthal anchoring of a nematic liquid crystal on a grooved interface with anisotropic polar anchoring*

Zhou Xuan(周 璇)[a)b)], Zhang Zhi-Dong(张志东)[c)†],
Ye Wen-Jiang(叶文江)[c)], and Xuan Li(宣 丽)[a)b)]

[a)] *State Key Laboratory of Applied Optics, Changchun Institute of Optics, Fine Mechanics and Physics, Chinese Academy of Sciences, Changchun* 130033, *China*

[b)] *Graduate School of the Chinese Academy of Sciences, Beijing* 100049, *China*

[c)] *Department of Physics, Hebei University of Technology, Tianjin* 300401, *China*

(Received 23 June 2011; revised manuscript received 3 November 2011)

Zhang Y J *et al.* [Zhang Y J, Zhang Z D, Zhu L Z and Xuan L 2011 *Liquid Cryst.* **38** 355] investigated the effects of finite polar anchoring on the azimuthal anchoring energy at a grooved interface, in which polar anchoring was isotropic in the local tangent plane of the surface. In this paper, we investigate the effects of both isotropic and anisotropic polar anchoring on the surface anchoring energy in the frame of Fukuda *et al.*'s theory. The results show that anisotropic polar anchoring strengthens the azimuthal anchoring of grooved surfaces. In the one-elastic-constant approximation ($K_{11} = K_{22} = K_{33} = K$), the surface-groove-induced azimuthal anchoring energy is entirely consistent with the result of Faetti, and it reduces to the original result of Berreman with an increase in polar anchoring. Moreover, the contribution of the surface-like elastic term to the Rapini–Papoular anchoring energy is zero.

Keywords: azimuthal anchoring energy, surface grooves, anchoring isotropy, anchoring anisotropy

PACS: 61.30.Hn **DOI:** 10.1088/1674-1056/21/6/066104

1. Introduction

Surface anchoring of nematic liquid crystal (LC) is one of the most important properties of LCs, mainly because of its relevance to practical applications, including main current displays[1−3] and various non-display technologies, such as LC spatial light modulators.[4,5] A property of nematic LC is that the distribution of the director in the bulk of an LC slab is affected by the properly treated substrate surface, as well as by externally applied fields, such as electric and magnetic fields. The easiest way to achieve an LC alignment along the direction parallel to the surface is to rub the surface of a polymer layer in that direction, by which the smectic LC,[3,6] as well as the nematic LC, is successfully anchored. There are two underlying mechanisms of anchoring on rubbed surfaces. One is the inter-molecular interaction between the LC molecules and the polymer chains constituting the surface,[7−10] while the other is the effect of long-range elastic distortion induced by surface grooves or scratches created in the rubbing process. For the past decade, interest in the latter mechanism has been growing, since nanotechnology has rapidly developed and has made it possible to tailor microscopically grooved surfaces to realize various anchoring properties.[11−20]

The first theoretical studies on the contribution of elastic origin to the surface anchoring of an NLC in the presence of a nonflat surface were carried out by Berreman.[21] In his analysis, he considered a rubbed surface described by a sinusoidal wave with wave number $q = 2\pi/\lambda$ and amplitude A, where λ is the spatial periodicity of the surface. Under the assumption of the strong anchoring condition, i.e. the director $\boldsymbol{n}$, a unit vector describing the local orientation of a nematic LC, at the surface is always parallel to it, small amplitude limit ($Aq \ll 1$), and one-elastic-constant approximation ($K_{11} = K_{22} = K_{33} = K$), the surface azimuthal anchoring energy is proportional to $\sin^2\varphi$ (φ being the angle between the director at infinity and the direction of the surface grooves), and

*Project supported by the Natural Science Foundation of Hebei Province, China (Grant No. A2010000004), the National Natural Science Foundation of China (Grant No. 60736042), and the Key Subject Construction Project of Hebei Provincial University, China.

†Corresponding author. E-mail: zhidong_zhang@yahoo.cn

© 2012 Chinese Physical Society and IOP Publishing Ltd

it varies strongly with amplitude A and wave number q. Since Berreman's model is simple enough, it has served as a starting point for numerous subsequent theories,[22−31] as well as experimental studies[32−34] in this field. In particular, Fukuda *et al.*[29] re-examined the theoretical treatment of Berreman's model for the surface anchoring induced by grooves with infinite polar anchoring (strong anchoring) and argued that Berreman's assumption of negligibly small azimuthal distortion of the nematic is not valid. They showed that Berreman's model, considering azimuthal distortion, yields a surface anchoring energy proportional to $\sin^4\varphi$ and implies that the surface grooves alone cannot contribute to the surface anchoring coefficient in the usual Rapini–Papoular sense. Furthermore, they considered the contribution of surface-like elasticity characterized by K_{24} and showed that the surface-like elastic term is a non-zero contribution to the Rapini–Papoular anchoring energy.[30,31]

In addition, Faetti[22] and Zhang *et al.*[28] investigated the effects of finite polar anchoring at a grooved interface on the azimuthal anchoring energy in the frame of Berreman's theory and Fukuda *et al.*'s theory, respectively. However, the polar anchoring they assumed was completely isotropic in the local tangent plane of the surface. But for the grooved surface, the rubbing procedure leads to anisotropic surface topology and anisotropic interaction between LC molecules and the oriented polymer chains on the surface.[8−10]

In this paper, extending the work of Fukuda and Yan-Jun Zhang *et al.*, we are going to investigate the effects of not only the isotropic anchoring of a nematic LC with the substrate (polar anchoring), but also the anisotropic component of planar surface anchoring[10] on surface azimuthal anchoring energy.

2. Theoretical results

The Frank elastic energy density of a nematic LC can be described in terms of $\boldsymbol{n}$ as[1]

$$\begin{aligned} f_{\rm el} = {} & \frac{1}{2}[K_{11}(\nabla\cdot\boldsymbol{n})^2 + K_{22}(\boldsymbol{n}\cdot\nabla\times\boldsymbol{n})^2 \\ & + K_{33}(\boldsymbol{n}\times\nabla\times\boldsymbol{n})^2] \\ & - \frac{1}{2}K_{\rm s}\nabla\cdot[\boldsymbol{n}(\nabla\cdot\boldsymbol{n}) + \boldsymbol{n}\times(\nabla\times\boldsymbol{n})], \end{aligned} \quad (1)$$

where $K_{\rm s}$ is the surface-like elastic constant. When the distortion of the nematic from the uniform alignment (we take the x direction to be along this aligned director) is small enough,[29] the director $\boldsymbol{n}$ can be written as

$$\boldsymbol{n} = (\sqrt{1-n_y^2-n_z^2}, n_y, n_z) \approx (\,1, n_y, n_z), \quad (2)$$

where n_y and n_z are small quantities. The Frank elastic energy density up to quadratic order in n_y and n_z reads

$$\begin{aligned} F_{\rm el} = {} & \frac{1}{2}\int\{K_{11}(\partial_y n_y + \partial_z n_z)^2 + K_{22}(\partial_y n_z - \partial_z n_y)^2 \\ & + K_{33}[(\partial_x n_y)^2 + (\partial_x n_z)^2] \\ & - 2K_{\rm s}[(\partial_y n_y)(\partial_z n_z) - (\partial_y n_z)(\partial_z n_y)]\}\,{\rm d}r, \end{aligned} \quad (3)$$

where the last term amounts to surface-like elasticity.

Here, we consider a surface groove whose shape can be described by

$$z = \varsigma(x,y) = A\sin[q(x\sin\varphi + y\cos\varphi)], \quad (4)$$

where A and q have been defined above, and φ describes the angle between the groove direction and the x axis (see Fig. 1). We assume that $Aq \ll 1$ and a nematic LC is filled in the semi-infinite region $z > \varsigma(x,y)$. We further assume that the director at the surface tends to lie in the direction tangential to it as in Berreman's theory, and the preferred direction on the surface is along the grooves.

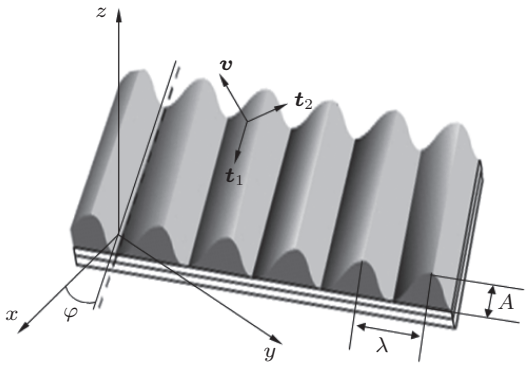


Fig. 1. Schematic representation of a sinusoidal groove surface with amplitude A and spatial periodicity λ. Here, φ is the angle between the x axis and the direction of the surface grooves, $\boldsymbol{t}_1$ is the unit vector along the grooves, $\boldsymbol{v}$ denotes the local unit vector perpendicular to the surface, and $\boldsymbol{t}_2 = \boldsymbol{v}\times\boldsymbol{t}_1$.

From Appendix A, the finite anchoring energy per unit area, taking into account both the direct anisotropic and isotropic interactions between the nematic LC molecules and the oriented polymer chains on the substrate surface, can be expressed by

$$f_{\rm s} = W_1(\boldsymbol{n}\cdot\boldsymbol{t}_1)^2 + W_3(\boldsymbol{n}\cdot\boldsymbol{v})^2, \quad (5)$$

where $\boldsymbol{n}$ is the nematic director at the surface, $\boldsymbol{t}_1$ is the unit vector along the grooves, $\boldsymbol{v}$ denotes the local unit vector perpendicular to the surface (see Fig. 1), W_1 is

the equivalent anisotropic anchoring strength coefficient related to director deviation in the local tangent plane from the limiting surface, and W_3 is the equivalent isotropic anchoring strength coefficient related to director deviation from the direction perpendicular to the surface. The finite anchoring energy of the surface is

$$\begin{aligned} F_{\rm s} = & \int W_1(\cos\varphi - \sin\varphi n_y)^2 \,{\rm d}S \\ & + \int W_3\{n_z - Aq\sin\varphi\cos[q(x\sin\varphi \\ & + y\cos\varphi)]\}^2 \,{\rm d}S. \end{aligned} \tag{6}$$

Using the full variational principle for $F_{\rm el}+F_{\rm s}$, we can derive the equilibrium conditions as follows:

$$\begin{aligned} & -K_{11}\partial_y(\partial_y n_y + \partial_z n_z) \\ & + K_{22}\partial_z(\partial_y n_z - \partial_z n_y) - K_{33}\partial_x^2 n_y = 0, \end{aligned} \tag{7}$$

$$\begin{aligned} & -K_{11}\partial_z(\partial_y n_y + \partial_z n_z) \\ & - K_{22}\partial_y(\partial_y n_z - \partial_z n_y) - K_{33}\partial_x^2 n_z = 0, \end{aligned} \tag{8}$$

together with the condition in the surface ($z = 0$):

$$n_y|_{z=0} = 0, \tag{9}$$

$$\begin{aligned} & K_{11}(\partial_y n_y + \partial_z n_z) - K_{\rm s}\partial_y n_y \\ = & \ 2W_3\{n_z - Aq\sin\varphi\cos[q(x\sin\varphi + y\cos\varphi)]\}, \end{aligned} \tag{10}$$

and with the ultimate conditions:

$$n_y|_{z=+\infty} = 0, \quad n_z|_{z=+\infty} = 0. \tag{11}$$

Equation (9) has been proposed by Wolff *et al.*[35] as an imposed boundary condition in the strong anchoring case, which induces the surface couple stress normal to the surface, while it is a natural result of the weak anchoring condition we considered. The details are given in Appendix B.

Using the general solutions of Eqs. (7) and (8) given by Wolff *et al.*,[35] we derive the following solutions consistent with the boundary conditions (9), (10), and (11) as follows:

$$\begin{aligned} n_z = & \ a_1\cos[q(x\sin\varphi + y\cos\varphi)]\,{\rm e}^{-qzg_2(\varphi)} \\ & + a_2\cos[q(x\sin\varphi + y\cos\varphi)]\,{\rm e}^{-qzg_1(\varphi)}, \end{aligned} \tag{12}$$

$$\begin{aligned} n_y = & \ d_1\sin[q(x\sin\varphi + y\cos\varphi)]\,{\rm e}^{-qzg_2(\varphi)} \\ & + d_2\sin[q(x\sin\varphi + y\cos\varphi)]\,{\rm e}^{-qzg_1(\varphi)}, \end{aligned} \tag{13}$$

where

$$a_1 = \frac{-Aq\sin\varphi\cos^2\varphi/(g_1(\varphi)g_2(\varphi) - \cos^2\varphi)}{1+\chi(\varphi)}, \tag{14}$$

$$a_2 = -\frac{g_1(\varphi)g_2(\varphi)}{\cos^2\varphi}a_1, \tag{15}$$

$$d_1 = \frac{g_2(\varphi)}{\cos\varphi}a_1, \tag{16}$$

$$d_2 = -\frac{g_2(\varphi)}{\cos\varphi}a_1, \tag{17}$$

with

$$\chi(\varphi) = \frac{qK_{33}}{2W_3}\left(\frac{g_2(\varphi)\sin^2\varphi}{g_1(\varphi)g_2(\varphi) - \cos^2\varphi}\right), \tag{18}$$

$$g_i(\varphi) = \sqrt{\cos^2\varphi + (K_{33}/K_{ii})\sin^2\varphi} \quad (i = 1, 2). \tag{19}$$

Now, the surface couple stress normal to the surface is[35]

$$\begin{aligned} \left.\frac{\partial g}{\partial n_{y,z}}\right|_{z=0} = & \ K_{\rm s}\partial_y n_z - K_{22}(\partial_y n_z - \partial_z n_y) \\ & + 2W_1\sin\varphi\cos\varphi \\ = & \ qK_{22}d_1\sin[q(x\sin\varphi + y\cos\varphi)] \\ & \times [g_1(\varphi) - g_2(\varphi)] - (K_{\rm s} - K_{22}) \\ & \times q(a_1 + a_2)\cos\varphi\sin[q(x\sin\varphi + y\cos\varphi)] \\ & + 2W_1\sin\varphi\cos\varphi, \end{aligned} \tag{20}$$

where $g = f_{\rm el} + f_{\rm s}$.

Substituting Eqs. (12) and (13) into expression $F_{\rm el} + F_{\rm s}$, after some calculations, we can obtain the total energy per unit surface area at angle φ, i.e. $F_{\rm sur}(\varphi)$. The surface azimuthal anchoring energy $w_{\rm a}(\varphi)$, which is defined by $F_{\rm sur}(\varphi) - F_{\rm sur}(0)$, is

$$\begin{aligned} w_{\rm a}(\varphi) = & \left[\frac{\frac{1}{4}K_{33}A^2q^3g_2(\varphi)\sin^4\varphi}{g_1(\varphi)g_2(\varphi) - \cos^2\varphi}\right. \\ & \left. + \frac{1}{2}W_3A^2q^2\sin^2\varphi\chi^2(\varphi)\right] \\ & \times \frac{1}{[1+\chi(\varphi)]^2} - W_1\sin^2\varphi, \end{aligned} \tag{21}$$

in which the last term $-W_1\sin^2\varphi$ is not the effect of the surface groove, and the surface-groove-induced azimuthal anchoring energy is

$$\begin{aligned} w_{\rm g}(\varphi) = & \left[\frac{\frac{1}{4}K_{33}A^2q^3g_2(\varphi)\sin^4\varphi}{g_1(\varphi)g_2(\varphi) - \cos^2\varphi}\right. \\ & \left. + \frac{1}{2}W_3A^2q^2\sin^2\varphi\chi^2(\varphi)\right] \\ & \times \frac{1}{[1+\chi(\varphi)]^2}. \end{aligned} \tag{22}$$

3. Discussion

The anchoring energy due to the direct interaction of the LC with the substrate can be considered to be strong when $qK_{33}/(2W_3) \ll 1$. From Eqs. (14)–(17), we can obtain

$$a_1 = -\frac{Aq\sin\varphi\cos^2\varphi}{g_1(\varphi)g_2(\varphi) - \cos^2\varphi}, \quad a_2 = -\frac{g_1(\varphi)g_2(\varphi)}{\cos^2\varphi}a_1,$$

$$d_1 = \frac{g_2(\varphi)}{\cos\varphi}a_1, \quad d_2 = -\frac{g_2(\varphi)}{\cos\varphi}a_1, \tag{23}$$

$$n_z = -\frac{Aq\sin\varphi\cos^2\varphi}{g_1(\varphi)g_2(\varphi)-\cos^2\varphi}\cos[q(x\sin\varphi+y\cos\varphi)] \times\left[\mathrm{e}^{-qzg_2(\varphi)}-\frac{g_1(\varphi)g_2(\varphi)}{\cos^2\varphi}\mathrm{e}^{-qzg_1(\varphi)}\right], \tag{24}$$

$$n_y = -\frac{Aq\sin\varphi\cos\varphi g_2(\varphi)}{g_1(\varphi)g_2(\varphi)-\cos^2\varphi}\sin[q(x\sin\varphi+y\cos\varphi)] \times[\mathrm{e}^{-qzg_2(\varphi)}-\mathrm{e}^{-qzg_1(\varphi)}]. \tag{25}$$

The surface-groove-induced azimuthal anchoring energy per unit surface area with strong polar anchoring can be obtained by Eq. (22) as

$$w_{\mathrm{g}}(\varphi) = \frac{1}{4}K_{33}A^2q^3\sin^4\varphi g_2(\varphi)/(g_1(\varphi)g_2(\varphi)-\cos^2\varphi). \tag{26}$$

In the one-elastic-constant approximation, that is $K_{11}=K_{22}=K_{33}=K$, equations (24)–(26) reduce to

$$n_z = Aq\sin\varphi\cos[q(x\sin\varphi+y\cos\varphi)]\,\mathrm{e}^{-qz}, \tag{27}$$

$$n_y = 0, \tag{28}$$

$$w_{\mathrm{g}}(\varphi) = \frac{1}{4}KA^2q^3\sin^2\varphi. \tag{29}$$

Equations (27)–(29) are consistent with the original results given by Berreman.[21]

In the one-elastic-constant approximation, that is $K_{11}=K_{22}=K_{33}=K$ and finite anchoring case, equation (22) reduces to

$$w_{\mathrm{g}}(\varphi) = \left[\left(\frac{1}{4}KA^2q^3+\frac{1}{2}W_3A^2q^2\chi_0^2\right)\Big/(1+\chi_0)^2\right]\sin^2\varphi, \tag{30}$$

where $\chi_0 = qK/(2W_3)$ is the value of $\chi(\varphi)$ under the condition of $K_{11}=K_{22}=K_{33}=K$. Equation (30) is the result given by Faetti.[22] We find that the surface-groove-induced azimuthal anchoring energy is proportional to $\sin^2\varphi$ and independent of the surface-like elastic constant K_{s}, which is different from the results provided by Fukuda *et al.*[30]

To see the effect of finite anchoring energy, we derive the rescaled anchoring energy $w_{\mathrm{g}}(\varphi)/(KA^2q^3/4)$ under one-constant approximation ($K_{11}=K_{22}=K_{33}=K$):

$$w_{\mathrm{g}}(\varphi)/(KA^2q^3/4) = \frac{1}{1+qK/(2W_3)}\sin^2\varphi. \tag{31}$$

For comparison, we plot in Fig. 2 Zhang *et al.*'s rescaled anchoring energy for $K_{\mathrm{s}}=0$[28] and ours (Eq. (31)) for various values of $qK/(2W_3)$. It is shown that with strong polar anchoring ($qK/(2W_3)\ll 1$), our result is the original result of Berreman, i.e. $w_{\mathrm{g}}(\varphi)\propto\sin^2\varphi$, while Zhang *et al.*'s anchoring energy is the result of Fukuda *et al.*,[29] i.e., $w_{\mathrm{g}}(\varphi)\propto\sin^4\varphi$. With the weak anchoring strength decreasing (we choose $qK/(2W_3)=1$ and $qK/(2W_3)=3$), and our result tends to be consistent with the result of Zhang *et al.* for $K_{\mathrm{s}}=0$. Furthermore, we can see that with the polar anchoring strength decreasing, the rescaled anchoring energy decreases more and more.

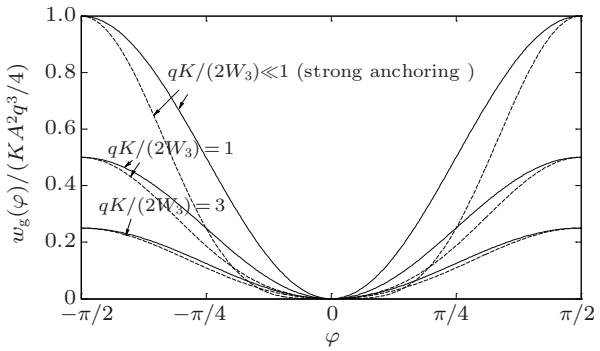


Fig. 2. Our rescaled anchoring energy (solid line) and that of Yan-Jun Zhang (dashed line) for $K_{\mathrm{s}}=0$ as a function of φ, assuming $K_{11}=K_{22}=K_{33}=K$.

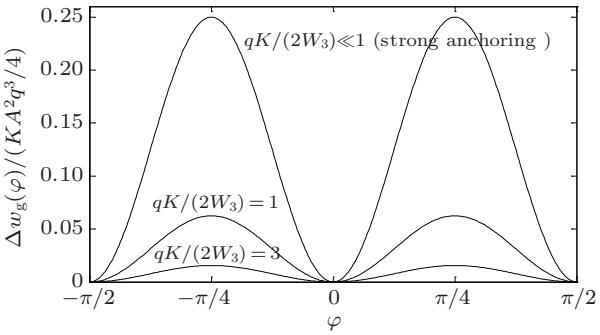


Fig. 3. The differences in rescaled anchoring energy between ours and Zhang *et al.*'s, each as a function of φ for various values of $qK/(2W_3)$, under the assumption of $K_{11}=K_{22}=K_{33}=K$.

To see the effects of anisotropic anchoring on azimuthal anchoring energy clearly, we plot in Fig. 3 and Fig. 4 the difference in rescaled anchoring energy between ours (using superscript aniso) and Zhang *et al.*'s (using superscript iso), i.e., $\Delta w_{\mathrm{g}}(\varphi)/(KA^2q^3/4) = w_{\mathrm{g}}(\varphi)^{(\mathrm{aniso})}/(KA^2q^3/4) - w_{\mathrm{g}}(\varphi)^{(\mathrm{iso})}/(KA^2q^3/4)$. In Fig. 3, it is shown that the difference is always positive, which means that our anchoring energy is always higher than Zhang *et al.*'s. In other words, the anisotropic anchoring strengthens the azimuthal anchoring energy of grooved surfaces. In addition, Fig. 4 shows that for a certain φ ($\varphi\neq 0,\ \pi/2$), the difference increases with increasing polar anchoring strength. In fact, our theory confirms that for the anisotropic

grooves induced by polymer stretching along the rubbing direction (stretch-induced anisotropy and mechanical damage-induced grooves) in industrial production, the anchoring effects are strengthened.

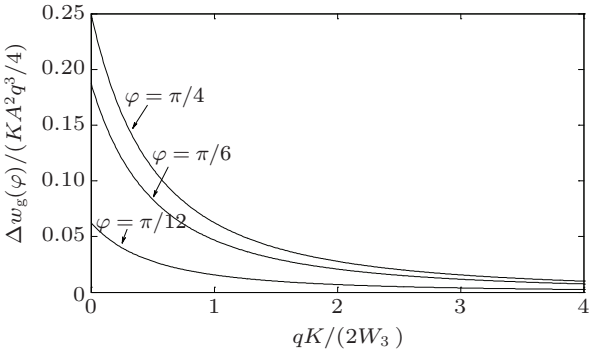


Fig. 4. The differences in rescaled anchoring energy between ours and Zhang *et al.*'s, each as a function of $qK/(2W_3)$ for various values of φ under the assumption of $K_{11} = K_{22} = K_{33} = K$.

In order to introduce the Rapini–Papoular[36] anchoring strength W on the easy axis $\varphi = 0$, defined by $w_g = \frac{1}{2}W\varphi^2$, we derive the second derivative of $w_g(\varphi)$ at $\varphi = 0$ as

$$W = \frac{A^2q^3\dfrac{K_{11}K_{22}}{K_{11}+K_{22}} + W_3A^2q^2\left(\dfrac{qK_{33}}{2W_3}\right)^2}{\left(1+\dfrac{qK_{33}}{2W_3}\right)^2}. \quad (32)$$

For $qK_{33}/2W_3 \ll 1$ (strong polar anchoring), equation (32) reduces to

$$W_0 = A^2q^3\frac{K_{11}K_{22}}{K_{11}+K_{22}}. \quad (33)$$

From Eq. (32), we find that the Rapini–Papoular anchoring strength W depends on the value of W_3, which is consistent with that in Ref. [28]. In contrast to the results in Refs. [28] and [30], it does not depend on the surface-like elastic term. Through simple analysis, we can conclude that the independence of W on the surface-like elastic term results from the fixed boundary condition of $n_y|_{z=0} = 0$.

4. Conclusion

In this paper, extending the work of Fukuda and Zhang Y J *et al.*, we investigated the surface-groove-induced azimuthal anchoring energy at a grooved interface with both isotropic and anisotropic anchoring. In the relatively strong anisotropic anchoring case, i.e., $2W_1$ is on the order of $K_{22}q$ and cannot be neglected, in order to obtain the solutions of n_y and n_z, a fixed condition on the surface, i.e., $n_y|_{z=0} = 0$, is naturally required, which induces the nonzero surface couple stress to be normal to the surface. The results show that finite anisotropic anchoring leads to a surface-groove-induced azimuthal anchoring energy (Eq. (22)) that is different from the result given in Ref. [28]. Compared with isotropic polar anchoring, the azimuthal anchoring for the anisotropic grooves is strengthened. Moreover, in the one-elastic-constant approximation, the surface-groove-induced azimuthal anchoring energy is consistent with the result of Faetti and reduces to the original result of Berreman with strong polar anchoring. In addition, we studied the Rapini–Papoular anchoring strength and found that under our assumption, the contribution of the surface-like elastic term to Rapini–Papoular anchoring energy is zero.

Appendix A

The tensor description of surface anchoring per unit area of LC is[37]

$$f_s = \sum_{\alpha,\beta} W_{\alpha\beta}(r)n_\alpha n_\beta, \quad (A1)$$

where $W_{\alpha\beta}(r)$ is the traceless symmetrical local anchoring tensor, which is diagonal with eigenvalues W_{11}, W_{22}, and W_{33} in the eigen frame. The tensor approach allows us to consider both the homogeneous and inhomogeneous parts of anchoring.

In the eigen frame of our grooved surface $(\boldsymbol{t}_1, \boldsymbol{t}_2, \boldsymbol{v})$, the finite anchoring energy per unit area can be expressed as

$$f_s = W_{11}(\boldsymbol{n}\cdot\boldsymbol{t}_1)^2 + W_{22}(\boldsymbol{n}\cdot\boldsymbol{t}_2)^2 + W_{33}(\boldsymbol{n}\cdot\boldsymbol{v})^2, \quad (A2)$$

where $\boldsymbol{t}_1$ is the unit vector along the grooves, $\boldsymbol{t}_2$ is the local geometrical tangent to the profile, and $\boldsymbol{v}$ denotes the local unit vector perpendicular to the surface (see Fig. 1 in the text).

As $\boldsymbol{t}_1$, $\boldsymbol{t}_2$, and $\boldsymbol{v}$ are mutually orthonormal, we have $(\boldsymbol{n}\cdot\boldsymbol{t}_1)^2 + (\boldsymbol{n}\cdot\boldsymbol{t}_2)^2 + (\boldsymbol{n}\cdot\boldsymbol{v})^2 = 1$, and then equation (A2) can be rewritten as

$$f_s = (W_{11}-W_{22})(\boldsymbol{n}\cdot\boldsymbol{t}_1)^2 + (W_{33}-W_{22})(\boldsymbol{n}\cdot\boldsymbol{v})^2 + W_{22}. \quad (A3)$$

If setting $W_1 = W_{11}-W_{22}$, $W_3 = W_{33}-W_{22}$ (here, W_1 and W_3 are the equivalent anisotropic and isotropic anchoring strength coefficients, respectively), and neglecting the W_{22} term, the finite anchoring energy per

unit area is obtained as

$$f_{\rm s} = W_1(\boldsymbol{n}\cdot\boldsymbol{t}_1)^2 + W_3(\boldsymbol{n}\cdot\boldsymbol{v})^2. \tag{A4}$$

Appendix B

Using the full variational principle for $F_{\rm el}+F_{\rm s}$, we can derive the equilibrium conditions given by Eqs. (7) and (8) in the text, together with the condition at the surface ($z=0$), as follows:

$$\begin{aligned}&\{K_{11}(\partial_y n_y+\partial_z n_z)-K_{\rm s}\partial_y n_y\\ &-2W_3\{n_z-Aq\sin\varphi\cos[q(x\sin\varphi+y\cos\varphi)]\}\}\delta n_z\\ &+[K_{\rm s}\partial_y n_z-K_{22}(\partial_y n_z-\partial_z n_y)\\ &+2W_1\sin\varphi(\cos\varphi-\sin\varphi n_y)]\delta n_y=0,\end{aligned} \tag{B1}$$

and with the ultimate conditions

$$n_y|_{z=+\infty}=0,\quad n_z|_{z=+\infty}=0. \tag{B2}$$

If no condition is imposed on n_y and n_z, equation (B1) can be written as

$$\begin{aligned}&K_{11}(\partial_y n_y+\partial_z n_z)-K_{\rm s}\partial_y n_y\\ &-2W_3\{n_z-Aq\sin\varphi\cos[q(x\sin\varphi\\ &+y\cos\varphi)]\}=0,\end{aligned} \tag{B3}$$

$$\begin{aligned}&K_{\rm s}\partial_y n_z-K_{22}(\partial_y n_z-\partial_z n_y)\\ &+2W_1\sin\varphi(\cos\varphi-\sin\varphi n_y)=0.\end{aligned} \tag{B4}$$

Equation (B4) denotes vanishing couple stress normal to the surface ($\frac{\partial g}{\partial n_{y,z}}\big|_{z=0}=0$), where $g=f_{\rm el}+f_{\rm s}$, with $f_{\rm el}$ and $f_{\rm s}$ given by Eqs. (1) and (5), respectively.

Using the general solutions of the equilibrium conditions given by Wolff *et al.*,[35] we derive the solutions consistent with the boundary conditions (B2) and (B3) as follows:

$$\begin{aligned}n_z=&a_1\cos[q(x\sin\varphi+y\cos\varphi)]\,{\rm e}^{-qzg_2(\varphi)}\\ &+a_2\cos[q(x\sin\varphi+y\cos\varphi)]\,{\rm e}^{-qzg_1(\varphi)},\end{aligned} \tag{B5}$$

$$\begin{aligned}n_y=&d_1\sin[q(x\sin\varphi+y\cos\varphi)]\,{\rm e}^{-qzg_2(\varphi)}\\ &+d_2\sin[q(x\sin\varphi+y\cos\varphi)]\,{\rm e}^{-qzg_1(\varphi)},\end{aligned} \tag{B6}$$

with

$$\frac{d_1}{a_1}=\frac{g_2(\varphi)}{\cos\varphi},\quad \frac{d_2}{a_2}=\frac{\cos\varphi}{g_1(\varphi)}. \tag{B7}$$

Substituting Eqs. (B5) and (B6) into Eq. (B4), we can obtain

$$\begin{aligned}&[(a_1+a_2)(K_{\rm s}-K_{22})q\cos\varphi\\ &+K_{22}q(g_2(\varphi)d_1+g_1(\varphi)d_2)\\ &+2W_1(d_1+d_2)]\sin(p_1x+p_2y)\\ &=2W_1\sin\varphi\cos\varphi.\end{aligned} \tag{B8}$$

From Eq. (B8), we find that if $2W_1$ is on the order of qK_{22} and cannot be neglected, Eq. (B8) (or Eq. (B4)) cannot be satisfied, in other words, there are no solutions of n_y and n_z consistent with the boundary conditions (B2)–(B4) simultaneously if no condition is imposed. This naturally requires a fixed boundary condition for n_y, i.e. $n_y|_{z=0}=0$, which requires that δn_y in Eq. (B1) must be set to be zero and induce the nonzero surface couple stress normal to the surface, i.e.

$$\left.\frac{\partial g}{\partial n_{y,z}}\right|_{z=0}\neq 0.$$

Since no condition is imposed on n_z, equation (B1) then results in an additional boundary condition at the surface ($z=0$):

$$\begin{aligned}&K_{11}(\partial_y n_y+\partial_z n_z)-K_{\rm s}\partial_y n_y\\ &-2W_3\{n_z-Aq\sin\varphi\cos[q(x\sin\varphi+y\cos\varphi)]\}=0.\end{aligned} \tag{B9}$$

References

[1] de Gennes P G and Prost J 1993 *The Physics of Liquid Crystals* 2nd edn. (Oxford: Oxford University Press)

[2] Jerome B 1991 *Rep. Prog. Phys.* **54** 391

[3] Takatoh K, Hasegawa M, Koden M, Itoh N, Hasegawa R and Sakamoto M 2005 *Alignment Technologies and Applications of Liquid Crystal Devices* (Oxon: Taylor & Francis)

[4] Kriezis E E, Parry-Jones L A and Elston S J 2003 *Optical Properties and Applications of Ferroelectric and Antiferroelectric Liquid Crystals*, in: *Optical Applications of Liquid Crystals*, ed. Vicari L (London: Institute of Physics Publishing)

[5] Bai F Z and Rao C H 2010 *Acta Phys. Sin.* **59** 8280 (in Chinese)

[6] Li W C, Liu Y G and Xuan L 2011 *Acta Phys. Sin.* **60** 046101 (in Chinese)

[7] Ishihara S, Wakemoto H, Nalazima K and Matsuo Y 1989 *Liq. Cryst.* **4** 669

[8] Geary J M, Goodby J W, Kmetz A R and Patel J S 1987 *J. Appl. Phys.* **62** 4100

[9] Cheng J and Boyd G D 1979 *Appl. Phys. Lett.* **35** 444

[10] Barbero G, Gliozzi A S and Scalerandi M 2008 *J. Appl. Phys.* **104** 094903

[11] Kim J H, Yoneya M, Yamamoto J and Yokoyama H 2001 *Appl. Phys. Lett.* **78** 3055

[12] Wen B and Rosenblatt C 2001 *J. Appl. Phys.* **89** 4747

[13] Zhang B, Lee F K, Tsui O K C and Sheng P 2003 *Phys. Rev. Lett.* **91** 215501

[14] Honma M, Yamamoto K and Nose T 2004 *J. Appl. Phys.* **96** 5415

[15] Lee F K, Zhang B, Sheng P, Kwok H S and Tsui O K C 2004 *Appl. Phys. Lett.* **85** 5556

[16] Varghese S, Crawford G P, Bastiaansen C W M, de Bore D K G and Broer D J 2005 *Appl. Phys. Lett.* **86** 181914

[17] Yeung F S, Ho J Y, Li Y W, Xie F C, Tsui O K, Sheng P and Kwok H S 2006 *Appl. Phys. Lett.* **88** 051910
[18] Yeung F S and Kwok H S 2006 *Appl. Phys. Lett.* **88** 063505
[19] Gwag J S, Fukuda J, Yoneya M and Yokoyama H 2007 *Appl. Phys. Lett.* **91** 073504
[20] Guan R H 2011 *Acta Phys. Sin.* **60** 016105 (in Chinese)
[21] Berreman D W 1972 *Phys. Rev. Lett.* **28** 1683
[22] Faetti S 1987 *Phys. Rev.* A **36** 408
[23] Fournier J B and Galatola P 1999 *Phys. Rev.* E **60** 2404
[24] Elgeti J and Schmid F 2005 *Eur. Phys. J.* E **18** 407
[25] Harnau L, Kondrat S and Poniewierski A 2007 *Phys. Rev.* E **76** 051701
[26] Barbero G, Gliozzi A S, Scalerandi M and Evangelista L R 2008 *Phys. Rev.* E **77** 051703
[27] Wen B, Mahajan M P and Rosenblatt C 2000 *Appl. Phys. Lett.* **76** 1240
[28] Zhang Y J, Zhang Z D, Zhu L Z and Xuan L 2011 *Liq. Cryst.* **38** 355
[29] Fukuda J, Yoneya M and Yokoyama H 2007 *Phys. Rev. Lett.* **98** 187803
[30] Fukuda J, Yoneya M and Yokoyama H 2007 *Phys. Rev. Lett.* **99** 139902(E)
[31] Fukuda J, Gwag J S, Yoneya M and Yokoyama H 2008 *Phys. Rev.* E **77** 011702
[32] Lee E S, Better P, Miyashita T, Uchida T, Kano M, Abe M and Sugawara K 1993 *Jpn. J. Appl. Phys.* Part 2 **32** L1436
[33] Newsome C J, O'Neill M, Farley R J and Bryan-Brown G P 1998 *Appl. Phys. Lett.* **72** 2078
[34] Barberi R, Dozov I, Giocondo M, Iovane M, Martinot-Lagarde Ph, Stoenescu D, Tonchev S and Tsonev L V 1998 *Eur. Phys. J.* B **6** 83
[35] Wolff U, Greubel W and Krüger H 1973 *Mol. Cryst. Liq. Cryst.* **23** 187
[36] Rapini A and Papoular M 1969 *J. Phys.* (Pairs) *Colloq.* **30** C4-54
[37] Shiyanovskii S V, Glushchenko A, Reznikov Yu, Lavrentovich O D and West J L 2000 *Phys. Rev.* E **62** 1477